Electron-lattice interaction and structural stability of the oxy-borate $Co_3O_2BO_3$

M. Matos

Departamento de Física, PUC-Rio, Gávea, CEP 22453-970,

Caixa Postal 38071, Rio de Janeiro, RJ, Brazil

A theoretical study is carried out in the homometallic mixed valent ludwigite $Co_3O_2BO_3$ using a modified tight binding methodology. The study focuses on the electronic properties of bulk, 1D and molecular units to describe differences between $Co_3O_2BO_3$ and another homometallic ludwigite, $Fe_3O_2BO_3$. The latter is known to present a structural instability which has not been found in $Co_3O_2BO_3$. Our results show that bulk band structures present no significant differences. Differences are found in the calculation of 1D stripes formed by $3^+2^+3^+$ triads, owed to different $3d$ occupancy of Fe and Co cations. Conditions for 1D semiconducting transport observed in $Fe_3O_2BO_3$ are not present in $Co_3O_2BO_3$. More important differences were found to be related to local octahedral geometry. Larger distortions in $Co_3O_2BO_3$ lead to higher $2^+ \rightarrow 3^+$ hopping barriers in the triads and consequent localization of charge. In $Fe_3O_2BO_3$, site equivalence provides easy paths for inter-cation hopping. It is then suggested that local geometry of the cation sites is the main cause of differences in these two compounds; dimerization in the triads, which characterizes the structural change in $Fe_3O_2BO_3$, could be structurally hindered in $Co_3O_2BO_3$. An analogy is made with two mixed-valent *warwickites*, Fe_2OBO_3 and Mn_2OBO_3, which show the same structural stability/site equivalence relationship.

PACS numbers:

I. INTRODUCTION

Ludwigite is an oxyborate with formula unit $M'_2MO_2BO_3$ in which divalent and trivalent metals M' and M are found inside 4 non equivalent edge-sharing oxygen octahedra, forming zig-zag planes mutually linked through BO_3 trigonal groups[1]. Fe and Co homometallic ludwigites are mixed valent compounds and were synthesized for the first time about two decades ago[2, 3]. $Fe_3O_2BO_3$ turned out to be the most challenging compound of the ludwigite family[4–9]. In the last few years increasing interest has been devoted to this material, motivated by its complex electronic, magnetic and transport properties and to a broad (150 to 300K) orthorhombic-orthorhombic structural change[10, 11]. Its main effect involves a distortion in a triad of Fe^{3+}-Fe^{2+}-Fe^{3+} cations with small $(2.6-2.9Å)$ inter-atomic distances. The pilling up of Fe triads along the short orthorhombic c axis has an almost independent 1D character in many respects and has been referred to as a 3LL

(three-leg-ladder) sub-structure, immersed in the corrugated 2D planes[12].

The structural transition in $Fe_3O_2BO_3$ has been theoretically investigated[12] and it has been suggested that its origin is associated to excitonic instabilities in the 3LL substruture. In another approach, based on orbital interactions, it was found that $3d$-$2p$ hybridization leads to small hopping barriers between Fe^{2+} and Fe^{3+}, favouring charge ordering at low temperatures[13]. To improve comprehension on the mechanisms involved, attention has been turned more recently to the other homo-metallic ludwigite, $Co_3O_2BO_3$[14, 15]. Despite the structural similarity between the two compounds, no conformational change was found in the latter. X-ray diffraction measurements, performed at low (105K) and high (293K) temperatures[14], showed the same orthorhombic structure, in the *Pbam* space group, found earlier by Norrestam et al.[3].

Magnetic properties present similarities and differences in the two materials. Both exhibit a low temperature magnetic order. $Co_3O_2BO_3$ becomes a weak ferromagnet or ferrimagnet below $\sim 45K$[14, 15] and $Fe_3O_2BO_3$ shows antiferromagnetic (AF) order below 50K[8, 11]. The Fe mixed-valent material has another AF phase, from 70K to 112K, in which only part of the atoms are magnetically aligned[7, 8]. Between 50 and 70K the passage from partial to total alignment of Fe spins (attained at 50K) is set in through a weak ferro-[8] or ferri-magnetic[7] order. The differences in magnetic and structural behavior of the two ludwigites would suggest that magnetism is involved in the structural change observed in $Fe_3O_2BO_3$. Nevertheless, the fact that in the iron material structural and magnetic transition temperatures are relatively far appart has been considered as an indication that the mechanism of atomic rearrangements is not directly and uniquely related to magnetism[14].

Electrical transport is more closely related to the structural transition in $Fe_3O_2BO_3$. In the low temperature phase, conductivity was found by different authors to be thermally activated, with activation energy of $\sim 0.2eV$[7, 9, 10]. At high temperature, the conductivity regime changes, with a steep decrease in the logarithmic derivative of the resistivity as a function of temperature[9]. For $Co_3O_2BO_3$, two mechanisms of electrical transport have been proposed[14, 15].

Charge distribution in $Fe_3O_2BO_3$ has been intensively studied through Mössbauer spectroscopy and a clear pattern was found in a temperature range as wide as $4K < T < 600K$[2, 6–8]. Below $\sim 50K$ complete ordering is found with all Fe atoms having valence +2 or +3, in the proportion $2 : 1$ as expected from stoichiometry. The trivalent metal sits preferentially at the borders of the triads. From this low temperature and up to $\sim 300K$, intermediate valence +2.5 is observed in the triad, indicating the presence of one $Fe^{2.5+} - Fe^{2.5+}$ pair and one trivalent Fe^{3+} atom per triad. This result indicates rapid hopping in one Fe dimer per triad. Above 300K the $Fe^{2.5+}$ disappears

from the Mössbauer spectra and again only divalent and trivalent Fe are found. Simultaneously, delocalization along c involving the extra Fe^{2+} electron was detected[6, 8]. The onset of 1D charge transport in the triad, along the c axis was previously suggested by Swinnea et al.[2]. Douvalis and colaborators[7] have observed a valence of $+2.75$ in the triad just before the disappearance of intermediate valences (at $\sim 270K$). This indicates that near the transition temperature, the extra Fe^{2+} electron gets more delocalized in the triad, so that one has one pair with $+2.75$ and one atom with $+2.5$. This delocalization inside the triad precedes 1D transport along the 3LL, in the non-dimerized orthorhombic structure.

An analogous behavior is found in mixed-valent warwickites, Fe_2OBO_3 and Mn_2OBO_3. The former undergoes a broad structural transition at $317K$, associated with a change in the conductivity regime and charge rearrangement in the low temperature phase[16, 17]. Mn_2OBO_3, however, presents no structural transition. In this compound, strong Jahn-Teller distortions of Mn^{3+} lead to a charge ordering state independent of temperature[16, 18, 19].

In the present paper, the extended Hückel tight binding (EHTB) method is used to investigate the electronic structure of $Co_3O_2BO_3$, using the high spin band hsf approach. Comparison is made with the electronic structure of the high temperature phase of $Fe_3O_2BO_3$, whose crystal structure is similar to that of the cobalt material. The calculations on $Fe_3O_2BO_3$ add to former calculations in the system[13, 22]. Norrestam et al.[3] gave a previous account of EHTB calculations on $Co_3O_2BO_3$. The hsf procedure prevents unphysical excesses of electron population in low lying $3d$ levels of the metal cation, allowing a correct account of basic structure-properties relationship. It is appropriate to narrow d band systems and showed to be particularly suitable to describe $Fe_3O_2BO_3$[13] and other oxy-borates[21, 23].

II. THEORY

The extended Hückel theory[20, 26] is widely known in the literature; here a brief summary of the relevant aspects of the theory, to the present study, is given. For the extended Hückel hamiltonian, diagonal terms H_{ii} and overlap integrals S_{ij} between atomic orbitals of the Slater type are needed. S_{ij} overlaps take into account the particular geometry of the system. The parameters used in the present study are chosen from ref.[25] and given as follows: (i) for O, $H_{2s,2s}=-32.3eV$, $H_{2p,2p}=-14.8eV$, $\zeta_{2s}=\zeta_{2p}=2.275$; (ii) for B, $H_{2s,2s}=-15.2eV$, $H_{2p,2p}=-8.5eV$, $\zeta_{2s}=1.3$, $\zeta_{2p}=1.2$; (iii) for Mn, $H_{4s,4s}=-9.75eV$, with $\zeta_{4s}=1.8$, $H_{4p,4p}=-5.89eV$ with $\zeta_{4p}=1.8$, $H_{3d,3d}=-11.67eV$, $\zeta_1=5.15$, $c_1=0.5113$, $\zeta_2=1.90$, $c_2=0.6659$; (iv)

for Fe, $H_{4s,4s}=-9.10eV$, with ζ_{4s}=1.9, $H_{4p,4p}=-5.32eV$ with ζ_{4p}=1.9, $H_{3d,3d}=-12.6eV$, $\zeta_1 = 5.35$, c_1=0.5505, ζ_2=2.00, c_2=0.6260; (v) for Co, $H_{4s,4s}=-9.21eV$, with ζ_{4s}=2.00, $H_{4p,4p}=-5.29eV$ with ζ_{4p}=2.00, $H_{3d,3d}=-13.18eV$, $\zeta_1 = 5.55$, c_1=0.5679, ζ_2=2.10, c_2=0.6059. Off-diagonal terms of the hamiltonian matrix, H_{ij}, are determined from weighted averages of H_{ii} and H_{jj} taking also into account S_{ij}[30]. Density of states are obtained from a mesh of 192 uniformly spread reciprocal lattice k points, whose set was found to be well suited to the oxyborate systems[22]. The Fermi level is defined as the highest occupied crystalline orbital. The high spin band filling (*hsf*) scheme has been discussed elsewhere[13]. An explanatory picture is that of minority spin electrons moving in a background of majority spin electrons. Mulliken population is used to calculate atomic charges.

All calculations were performed with bind[27] program and the graphics were drawn with viewkel[28], distributed as part of the YAeHMOP package.

III. CRYSTAL STRUCTURE

Fig.1 shows a polihedral drawing of the ludwigite structure seen along the c-axis. Sites 1,2 and 3 are preferentially occupied by divalent metals while metal site 4 is usually trivalent. Two-fold 1 and 2 plus four-fold 3 and 4 provide eight di- and four tri-valent sites, thus satisfying the unit cell stechiometry $(M_2'^{2+}M^{3+}B^{3+}O_5^{2-})_4$. The 4-2-4 triad is the basic unit that forms the 3LL 1D substructure, running paralel to the c-axis, mentioned above. Structure refinements of $Co_3O_2BO_3$ and of the 294K phase of $Fe_3O_2BO_3$ were made in the *Pbam* space group n. 55 [10, 14, 15]. Some structural parameters are given in Table 1, which contains an estimate of octahedral distortions Δ, given by the average of the difference $[(d_{M-O_i} - d_{av})/d_{av}]^2$, $i = 1, .., 6$, for each MO_6 group[29].
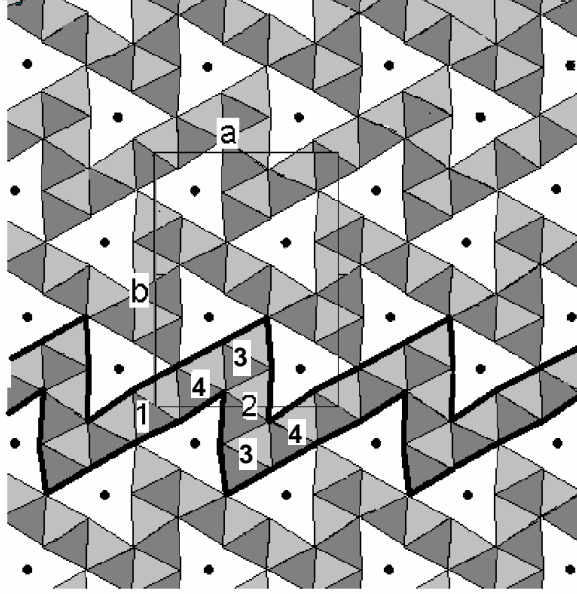
FIG. 1: The crystal structure of the ludwigite, seen along the hexagonal c-axis; Fe-triad: $4 - 2 - 4$.

	$Co_3O_2BO_3$	$Fe_3O_2BO_3$
Table 1 - Structure data of homometallic ludwigites		
Lattice parameters a,b,c, metal-oxygen average distances, metal-metal distances (in Å) and octahedral distortions Δ		
a	9.30	9.46
b	11.96	12.31
c	2.97	3.08
$d(M1-O)_{av}$	2.10	2.15
$10^3\Delta$	1.04	1.27
$d(M2-O)_{av}$	2.07	2.09
$10^3\Delta$	0.81	0.11
$d(M3-O)_{av}$	2.09	2.15
$10^3\Delta$	1.01	1.92
$d(M4-O)_{av}$	1.93	2.06
$10^3\Delta$	0.15	0.30
$d(M1-M4)$	3.01	3.10
$d(M2-M3)$	3.06	3.18
$d(M2-M4)$	2.75	2.79
$d(M3-M4)$	3.09	3.19
Data for $Fe_3O_2BO_3 \rightarrow \Delta$: this work; other: ref. [22]		

IV. RESULTS

The bulk (3D) and 3LL(1D) EHTB band structures of $Co_3O_2BO_3$ and $Fe_3O_2BO_3$ are shown in Fig.2 in the metal $3d$ energy range; band structure properties are given in Table 2. Oxygen $2p$ bands (not shown) appear at $\sim 0.9eV$ (Co ludwigite) and $\sim 1.5eV$ (Fe ludwigite) below the metal d bands. The two separate groups of bands, seen in Fig.2, come from the cubic d-splitting of the oxygen octahedral field and will be denoted t_{2g} and e_g. Two narrower t_{2g} bands are seen to be detached from the main group. They are characteristic of the ludwigite structure and come from strong metal-metal interactions in the triad, thus named σ and $\sigma*$[13, 31]. The 3LL(1D) $0.22eV$ semiconducting gap which appears in $Fe_3O_2BO_3$ (see Fig.2, fourth panel) has been associated to the electronic barrier responsible for the thermally activated behavior experimentally observed
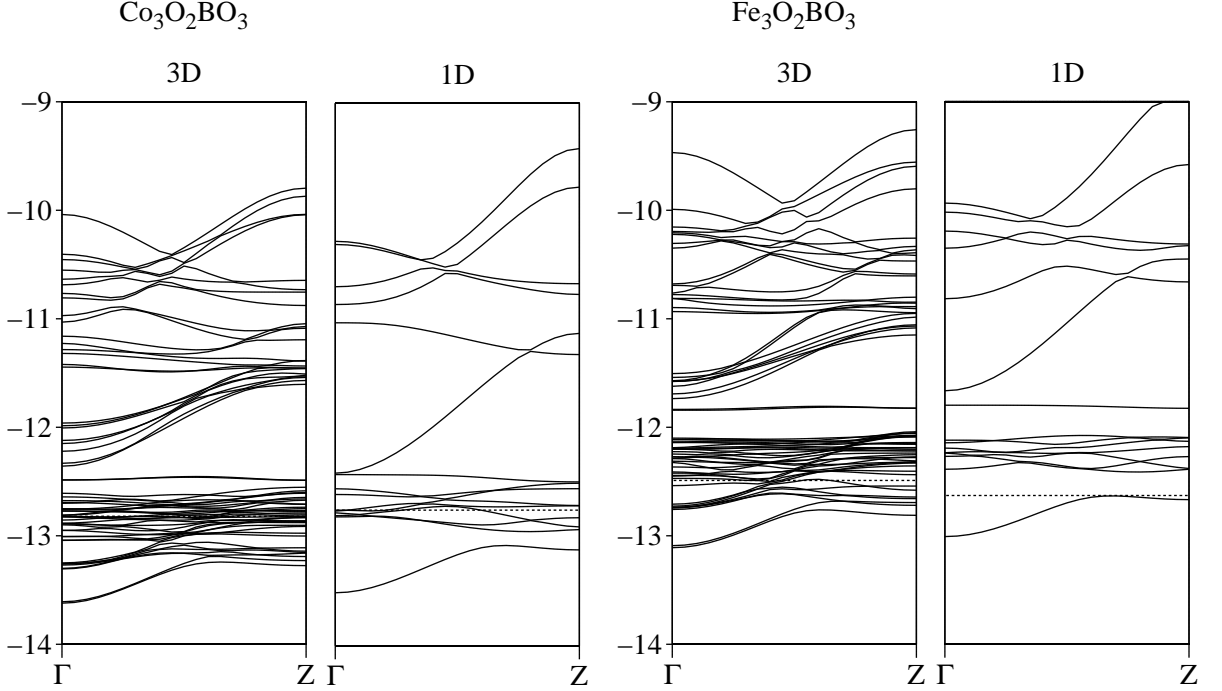
FIG. 2: The bulk and 1D (3LL) $3d$ bands of $Co_3O_2BO_3$ and $Fe_3O_2BO_3$, showing the σ and $\sigma*$ bands. Note the 1D gap above the Fermi level (doted line) in the Fe compound. Band structure of $Fe_3O_2BO_3$: see also refs.[13, 22].

in the iron ludwigite[13]. The calculated gap is in good agreement with the experimental value, estimated to be $\sim 0.2eV$[7, 9, 13]. Its existence is also confirmed by Mössbauer data which indicates the onset of 1D transport through the 1D stripe[6].

Co^{2+} ($3d^{5+2}$) and Co^{3+} ($3d^{5+1}$) give $8 \times 2 + 4 \times 1 = 20$ spin down electrons per unit cell, leading to 20/36 fractional occupancy of t_{2g} bands, larger than the 8/36 fraction of $Fe_3O_2BO_3$. Therefore, due to electron counting, the Fermi level of the cobalt ludwigite is raised; a significant effect of electron counting is the disapearance of the 1D gap of $Co_3O_2BO_3$. This constitutes an important difference between both materials, from which a different conductivity behavior could be expected. This point will be discussed below.

	$Co_3O_2BO_3$	$Fe_3O_2BO_3$
Table 2 - Calculated electronic structure properties. Energies in eV.		
E_F (1D)	-12.75	-12.63^*
E_F (3D)	-12.82	-12.49
δ_c (1D)	0.01	0.14
δ_c (3D)	0.09	0.07
1D gap	0	0.22
E_F: the hsf Fermi level; δ_c: the t_{2g}-e_g cubic splitting		
$*$: top of σ band		

In Table 3 are shown the calculated atomic charges. For consistency, one compares charge distribution in the crystal (3D) and the 3LL (1D) sub-system.

	$Co_3O_2BO_3^{(a)}$	$Fe_3O_2BO_3^{(b)}$
Table 3 - Metal charge distribution of $Co_3O_2BO_3$ and $Fe_3O_2BO_3$		
1D		
$q(M1)$	$-$	$-$
$q(M2)$	0.777	1.255
$q(M3)$	$-$	$-$
$q(M4)$	1.529	1.473
3D		
$q(M1)$	0.848	1.004
$q(M2)$	0.940	1.234
$q(M3)$	0.853	1.198
$q(M4)$	1.502	1.235
(a): this work; (b) ref. [13]		

Charge localization is clearly observed in $Co_3O_2BO_3$ in contrast with $Fe_3O_2BO_3$, where no significant distinction is obtained in $q(Fe)$ at different sites. In the former, calculated values of $q(Co1)$, $q(Co2)$ and $q(Co3)$ ($\sim 0.8 - 0.9$) and that of $q(Co4)$ (~ 1.5), lead one to associate the

former three to divalent and the latter to trivalent cations. Empirical estimates of cobalt oxidation state in $Co_3O_2BO_3$, using valence bond sums (vbs), provide for sites 1, 2 and 3, valences of 1.91, 2.06 and 1.98, respectively, consistent with 2+ cations and 2.73 for site 4, which can be associated to a 3+ oxidation state[14]. In the 1D sub-systems, the same delocalization/localization behavior is observed in the Co/Fe materials although, as expected, charges come out to be slightly more localized in both cases, due to lower dimensionality. Charge distribution is well correlated to the sizes of O octahedra, given in Table 2. While in $Co_3O_2BO_3$, 2+ octahedra are noticeably larger than 3+, in $Fe_3O_2BO_3$, the Fe triad sites, besides being smaller than those outside, are very similar, consistent with intermediate valence. As expected, the quantum mechanical calculated charges differ in absolute values from empirical estimates but the same trend is found in the charge distribution. In the next section, other effects associated to octahedral subunits are investigated.

A.   Monomers and dimers

Basic insight of electronic processes taking place in the physical system is obtained by examining structural sub-units such as *monomers* CoO_6, FeO_6 and *dimers* Co_2O_{10}, Fe_2O_{10}. It has already been shown that the density of states of oxy-borates are well reproduced by the electronic levels of the respective sub-units[21, 23, 30, 31]. This is related to the ionic character of the system. As the hopping barriers are small, $\sim 0.1eV$, we compare EHTB and more precise embedded cluster DFT calculations in the study of isolated subunits.

One considers first $M^{2+}O_6^{12-}$ and $M^{3+}O_6^{12-}$ isolated monomers ($M=Fe$, Co), carved out from the material's crystalline structure. In the high spin state of $Co^{2+/3+}$ ($3d^{5+2/5+1}$) there are 2/1 minority spins so that 2/1 molecular levels of the t_{2g} group are doubly occupied. For $Fe^{2+/3+}$ ($3d^{5+1/5}$) one has 1/0 minority spins in 1/0 t_{2g} levels. In Fig.3, the calculated t_{2g} molecular structure of the monomers is shown for the triad sites 2 and 4 of $Co_3O_2BO_3$ and $Fe_3O_2BO_3$. This is the energy range where comparison between sites is meaningful for the analysis. The occupied molecular orbital ($HOMO^\downarrow$) is indicated for each case ($Fe4$ is presented as a trivalent cation). Effects of geometrical distortions of the different oxygen octahedra are clearly seen to produce distinct degeneracy breaking of the 3-fold t_{2g} levels.

From Fig.3, two elementary paths for intersite electron transfer between adjacent monomers in the cobalt 4-2-4 triad can be indentified. One is from the $HOMO^\downarrow$ of $Co2$ to the $LUMO^\downarrow$ of $Co4$, namely $2 \Rightarrow 4$. The other path is the reverse, from the $HOMO^\downarrow$ of $Co4$ to the $LUMO^\downarrow$ of $Co2$, namely $4 \Rightarrow 2$. Along the c-axis there are two more $HOMO^\downarrow$-$LUMO^\downarrow$ paths, represented by

$2 \mapsto 2$ and $4 \mapsto 4$. In $Fe_3O_2BO_3$, there is just $2 \Rightarrow 4$ in the triad and $2 \mapsto 2$ along c, as there are no spin down electrons in the t_{2g} levels of the $Fe4$ monomer. Table 4 shows the inter-site transition energies $\Delta_{ij}=E_{LUMO_j^{\downarrow}}-E_{HOMO_i^{\downarrow}}$, from which energetic trends could be obtained.

Table 4 - Direct intersite $HOMO_i$-$LUMO_j$ transition energies Δ_{ij} in the triad. Energies in eV. ”U” parameter, discussed in the text.		
site pair i,j	$Co_3O_2BO_3$	$Fe_3O_2BO_3$
$2 \Rightarrow 4$	0.16	0.05
$4 \Rightarrow 2$	$-0.06 + $”2U”	-
$2 \mapsto 2$	$0.01 + $”U”	$0.04 + $”U”
$4 \mapsto 4$	$0.06 + $”U”	-

Effects of in-site electron-electron repulsion on inter-site transfer is qualitatively taken into account in Table 4 by hypothetical amounts ”U” and ”$2U$”, aiming to indicate differences which would arise upon changing the oxidation state of the pair. For instance, the $2 \Rightarrow 4$ jump changes the atoms oxidation states from $2^+, 3^+$ to $3^+, 2^+$, with no net effect, so that no repulsive amounts were added to the electron-lattice contribution to this jump ($0.16eV$ for Co and $0.05eV$ for the Fe ludwigite). On the other hand, the $4 \Rightarrow 2$ jump changes the pair oxidation states from $3^+, 2^+$ to $4^+, 1^+$, so that repulsion energy increases are represented by ”$2U$”. The $2 \mapsto 2$ jump changes the pair oxidation state from $2^+, 2^+$ to $3^+, 1^+$, thus an amount of $-$”U”$+$”$2U$”$=$”U” has been added. The analysis would suggest that electron hopping in $Co_3O_2BO_3$ deals with higher energetic cost than in $Fe_3O_2BO_3$.

It is possible to gain additional insight by investigating the electronic structure of molecular dimers, since dimerization is the essential physical mechanism of the structural transition in $Fe_3O_2BO_3$. As metal-metal interaction is directly influenced by oxygen ligands, one considers the subunits $Co_2Co_4O_{10}$ and $Fe_2Fe_4O_{10}$, which preserve the octahedral vicinity of the metal pair. In Fig.4, it is shown the calculated molecular orbital structure of these metal dimers, seen as built up from individual fragments MO_5; three t_{2g} levels of each fragment, $M2O_5$ and $M4O_5$, combine to form the six lower lying molecular orbital levels. As the constituent fragments have electronic

configurations corresponding to $Co^{2+/3+}$ and $Fe^{2+/3+}$, the three lowest (for Co) and one lowest (for Fe) dimer molecular orbitals (MO's) are occupied with spin down electrons.

One would expect more covalent dimers to be more likely to dimerize in the crystalline structure. Since energy levels of neighbor Fe monomers are closer to each other, when compared to Co monomers (see Fig.3), better conditions for dimerization are to be expected in $Fe_3O_2BO_3$. This is in fact confirmed by actual calculation. As the lowest dimer MO's are ligand $3d$-O_{2p} combinations, covalency could be estimated by means of minority spin density distribution in the subunits. Let $\rho_{E_i}(atom)$ be the atom-projected density of states in MO energy level E_i. The lower lying MO's $i = 1, 2, 3$ in Co and $i = 1$ in Fe subunits, contribute with $\rho_{E_i}(2)$ and $\rho_{E_i}(4)$, so that the ratio $r_{2,4}=[\sum_i \rho_{E_i}(2)]/[\sum_i \rho_{E_i}(4)]$ provides the degree of localization of minority spins within the dimer. Calculations give a density ratio of 5.6 for cobalt, significantly larger than the corresponding ratio found for Fe dimers; in the latter, $r_{2,4}=1.3$. Thus, in the dimer $Co2Co4O_{10}$, minority spin density is mainly localized around $Co2$, while in the $Fe2$-$Fe4$ dimers the extra spin spreads almost equaly among the two metals, a situation which favors dimerization, as compared with the Co compound.

Outside the triad, monomers 1 and 3 in $Co_3O_2BO_3$ have molecular electronic structures fairly equal to that of site 2, with the t_{2g} levels spreading between $-13eV$ and $-12.8eV$ below the corresponding levels of $Co4$. Thus, all Co^{2+} sites are structurally analogous, and distinct from Co^{3+}. In $Fe_3O_2BO_3$, metal sites 1 and 3 have t_{2g} levels spreading in the same energy range as that of the triad sites, but the 2+ configuration is slightly more stable.

V.   DISCUSSION

Charge distribution in Co and Fe homometallic ludwigites show localization in the former and delocalization in the latter. This difference is related to local distortions of the four oxygen octahedra which seem to determine specific conditions for conductivity paths. Electronic equivalence of Fe sites in the $Fe_3O_2BO_3$ triad is an important aspect of the difference between the electronic structure of the two materials.

Electronic structure equivalence of Fe^{2+} and Fe^{3+} monomers have also been found in the mixed valent Fe_2OBO_3 warwickite[21]. Taking into account that both Fe oxyborates have structural transitions associated to charge rearrangements - through dimerization in the ludwigite[6] and by means of a Wigner phase in the warwickite[16], one could establish a common behavior in these two materials. In both cases, easy paths for electron transfer between di- and tri-valent sites create instabilities in the charge distribution, which allows different arrangements. If other

stabilizing mechanisms are present, charge ordering/localization may occur in such conditions. In the Fe warwickite this is provided by coulombian repulsion between the extra electrons of Fe^{2+}, defining the Wigner crystal arrangement of the low temperature phase[16]. In the ludwigite, dimerization provides chemical stabilization. In a recent work, Vallejo et al.[34] have shown that local ferromagnetic ordering in the triad could strenghten $Fe2$-$Fe4$ bonds, contributing further to stabilize dimerization. It should be noted that in the other two mixed-valent oxyborates, $Co_3O_2BO_3$ and the warwickite Mn_2OBO_3, no structural transition has been observed. A similar theoretical analysis has found larger barriers for electron jump in the manganese compound, associated to Janh-Teller distortions[23].

Larger barriers for electron jump in $Co_3O_2BO_3$, found in the analysis above, would be consistent with a Mott like conductivity regime, as suggested by Ivanova et al.[15]. The band structure calculation of Fig.3 predicts, on the other hand, metallic behavior (see Fig.3), as suggested by Freitas et al.[14]. More experimental and theoretical studies are necessary to determine the electrical conductivity regime of $Co_3O_2BO_3$. The present investigation could provide some basic understanding of the role of electron-lattice interaction in the compound.

VI.   CONCLUSION

In this paper, a basic structure-property investigation is carried out in two homometallic ludwigites, $Co_3O_2BO_3$ and $Fe_3O_2BO_3$, by using the EHTB-*hsf* method. The band structures of $Co_3O_2BO_3$ and of two crystalline phases of $Fe_3O_2BO_3$ were found to be very similar, consistently with the structural similarity of the compounds. Different $3d$ occupancy of Co and Fe leads however to important differences in the electronic structures of both materials. In both compounds short metal-metal distances in the triad generate a separation of the lower t_{2g} band. However, due to electron occupancy, it is only in $Fe_3O_2BO_3$ that the separation constitutes a true 3LL semiconductor gap, consistently with experiment.

Calculations show that small differences in the local octahedral geometry at different sites lead to significant differences in the charge distribution of the two compounds. In agreement with Mössbauer results, electronic equivalence was observed between divalent and trivalent Fe cations in the triad, at both structural phases of $Fe_3O_2BO_3$. On the other hand, structural and electronic conditions for charge localization are obtained in $Co_3O_2BO_3$. The electronic structure of all relevant monomers and dimers were examined, showing that site non equivalence could create higher barriers for electron hopping in the cobalt ludwigite, hindering dimerization in this

compound. For $Fe_3O_2BO_3$, charge distribution instabilities, related to small hopping barriers, are suggested to play a relevant role in the structural transition observed for this material.

An analogy is made with the two mixed-valent warwickites, Fe_2OBO_3 and Mn_2OBO_3, since site equivalence in the former has been associated to the structural transition and changes in the conductivity regime, while, in the Mn compound, structural stability is associated with structural charge ordering. The nature of electrical conductivity in $Co_3O_2BO_3$ is briefly discussed.

For a complete understanding of the physics of the mixed-valent ludwigites, more experimental and theoretical work is necessary. The present results could provide a comprehensive understanding of important features related to electron-lattice interactions in these complex materials.

[1] Y. Takéuchi, Takéo Watanabe and T. Ito, 1950, Acta. Cryst., **3** 98-107; a detailed description of the ludwigite structure could be found in Howard W. Jaffe, 1996, "Crystal Chemistry and Refractivity", Dover,256-259.

[2] J.S. Swinnea and Hugo Steinfink, 1983, American Mineralogist, **68** 827-832.

[3] R. Norrestam, K. Nielsen, I. Sotofte and N. Thorup, 1989, Z. Kristallogr., **189** 33.

[4] J.P. Attfield, J. F. Clarke and D. A. Perkins, 1992, Physica B, **180-181** 581-584.

[5] J.C.Fernandes, R.B.Guimarães, M.A.Continentino, L.Ghivelder, and R.S.Freitas, 2000, Phys. Rev., **B61** R850-853.

[6] J. Larrea, D.R. Sánchez, F.J. Littest and E.M. Baggio-Saitovitch, 2001, J. Phys.: Cond. Matter, **13** L949-L954.

[7] A.P. Douvalis, A. Moukarika, T. Bakas, G. Kallias and V. Papaefthymiou, 2002, J. Phys.: Cond. Matt., **14** 3303-3320.

[8] J. Larrea, D.R. Sánchez, F.J. Littest, E.M. Baggio-Saitovitch, J.C.Fernandes, R.B.Guimarães and M.A.Continentino, 2004, Phys. Rev., **B70** 174452(1-8).

[9] J.C.Fernandes, R.B.Guimarães, M.A.Continentino, E.C. Ziemath, L. Walmsley, M. Monteverde, M. Núñez-Regueiro, J.-L. Tholence and J. Dumas, 2005, Phys. Rev., **B72** 075133(1-5).

[10] M.Mir, R.B.Guimarães, J.C.Fernandes, M.A.Continentino, A.C.Dorigueto, Y.P.Mascarenhas, J.Ellena, E.E.Castellano, R.S.Freitas and L.Ghivelder, 2001, Phys. Rev. Lett., **87** 147201(1-4); M. Mir, Jan Janczakb and Y. P. Mascarenhas, 2006, J. Appl. Cryst., **39**, 4245.

[11] P. Bordet and E. Suard, 2009, Phys. Rev. **B79**, 144408(1-7).

[12] A. Latgé and M.A. Continentino, 2002, Phys. Rev., **B66** 94113(1-5).

[13] M. Matos, 2004, J. Solid State Chem., vol.**177**, 4605-4615.

[14] D.C. Freitas, M.A.Continentino, R.B.Guimarães, J.C.Fernandes, J. Ellena and L.Ghivelder, 2008, Phys. Rev., **B77** 184422(1-8).

[15] N.B. Ivanova, A.D. Vasilév, D.A. Velikanov, N.V.Kazak, S.G. Ovchinnikov, G.A. Petrakovskii and V.V. Rudenko, 2007, Physics of the Solid State, **49** 651-653.

[16] J.P. Attfield, A.M.T. Bell, L.M.Rodriguez-Martinez, J.M. Greneche, R.J. Cernick, J.F. Clarke and D.A.Perkins, 1998, Nature (London), **396** 655-658.

[17] J.P. Attfield, A.M.T. Bell, L.M. Rodrigues-Martinez, J.M. Greneche, R. Retoux, M. Leblanc, R.J. Cernik, J. F. Clarke and D. A. Perkins, 1999, J. Mat. Chem., **9** 205-209.

[18] R. Norrestam, M. Kritikos and A. Sjödin, 1995, Journal of Sol. State Chem., **114** 311-316.

[19] R. J. Goff, A. J. Williams and J.P. Attfield, 2004, Phys. Rev., **B70** 014426 (1-5).

[20] R. Hoffmann, 1963, J. Chem. Phys.,**39** 1397-1412 ; M.-H. Whangbo and R. Hoffmann, 1978, J. Am. Chem. Soc., **100**, 6093-6098.

[21] M. Matos and R.B.Oliveira, 2006, J. Physics: Cond. Matt., **18** 8267-8280.

[22] M. Matos and A. X. Souza, 2005, Intern. J. of Quantum Chem., **103** 562-571.

[23] M. Matos and R.B.Oliveira, 2006, Int. J. Quantum Chem., **106** 2737-2746.

[24] M. Matos and L. Walmsley, 2006, J. Phys.: Condens. Matter, **18** 1793-1803.

[25] Tables of Parameters for Extended Hückel Calculations, collected by Santiago Alvarez, Universitat de Barcelona, 1993.

[26] R. Hoffmann, in *Solids and Surfaces*, VCH Publishers Inc., New York, 1988.

[27] G. A. Landrum and W. V. Glassey, bind (ver 3.0). bind is distributed as part of the YAeHMOP extended Hückel molecular orbital package and is freely available on the www at: http://sourceforge.net/projects/yaehmop.

[28] G. A. Landrum, viewkel (ver 3.0). viewkel is distributed as part of the YAeHMOP extended Hückel molecular orbital package and is freely available on the www at: http://sourceforge.net/projects/yaehmop.

[29] R. D. Shannon, 1976, Acta Crystallographica A, **32** 751.

[30] M.Matos, E.V. Anda, J.C. Fernandes and R.B. Guimarães, 2001, J. Mol. Struct. (THEOCHEM), **539** 181-190.

[31] M. Matos, R. Hoffmann, A. Latgé and E.V. Anda, 1996, Chemistry of Materials, **8** 2324-2330.

[32] M.-H. Whangbo, H.-J. Koo, J. Dumas and M.A.Continentino, 2002, Inorg. Chem., **41** 2193-2201.

[33] I. Leonov, A. N. Yaresco, V. N. Antonov, J.P. Attfield and V.I. Anisimov, 2005, Phys. Rev., **B72** 014407 (1-7).

[34] E. Vallejo and M. Avignon, 2006, Phys. Rev. Lett., **97** 217203(1-4)